Numerical modeling and validation of a Chemical Reactor Network for NH_3/H_2/air flames and theoretical evaluation of the Rich-Quench-Lean implementation

Francisco Manuel Freitas Mesquita Guimarães
francisco.m.guimaraes@tecnico.ulisboa.pt
Instituto Superior Técnico, Universidade de Lisboa, Portugal

December 2021

Abstract

Ammonia (NH_3) has emerged as an alternative fuel for important combustion applications. Its carbon-free chemical composition allows for zero-CO_2 burning, therefore preventing from relevant greenhouse gases emissions. Low reactivity, the emission of NO_x and unburnt NH_3, which is toxic, are the biggest issues concerning NH_3 combustion. Some drawbacks of the use of NH_3 as fuel - weak reactivity, low flame speed, high ignition delay time and hard flame stabilization - can be partially overcome by adding H_2. To study the most concerning combustion emissions of this type of mixture - NO_x, NH_3 and H_2 - the Chemical Reactor Network modeling method was chosen to model a swirl and bluff-body stabilized burner, for which experimental data on temperatures and chemical species is already documented in previous works. Thus, a model of Perfectly Stirred Reactors and a Plug-Flow Reactor was developed, taking into account aerodynamic and geometric characteristics of the burner and being able to predict temperature, pressure, residence time, chemical species and combustion efficiency. The model was validated against experiments and discrepancies are addressed. It shows good agreement with experiments on predicting qualitative trends related to variation of thermal input, equivalence ratio and NH_3 mole fraction in fuel. However it fails on predicting accurately quantitative values of NO_x, NH_3 and H_2, which is discussed. Finally, the model is extended to include a secondary air injection stage, to theoretically predict optimal conditions for a Rich-Quench-Lean combustor, a method used for the decreasing of NO_x, NH_3 and H_2 emissions, while securing high overall combustion efficiency.

Keywords: Alternative fuels, Ammonia, Hydrogen, Stabilized burner, Chemical Reactors Network, Rich-Quench-Lean.

1 Introduction

To study NH_3 enhanced with H_2 flame performance and emissions, Franco et al. [3] firstly presented a swirl and bluff-body stabilized burner for ammonia-hydrogen semi/quasi-premixed turbulent flames focusing on lean flame stabilization and temperature and emissions measurements and analysis. The authors did a quite detailed description on axial and radial lean flame temperature and emissions of NO and O_2 in several burner points for each one of five flames with different conditions.

For some of the analyzed flames mentioned above Rocha et al. [11] conducted Reynolds-Average Navier Stokes (RANS) simulations to study aerodynamics and mixing characteristics of the flow. The simulations are performed for chemistry turned off to represent isothermal flow profiles. In terms of flow fields the authors suggested the existence of three important recirculation zones, namely central recirculation zone (CRZ), inner recirculation zone (IRZ) and outer recirculation zone (ORZ), which interact with each other affecting thus the shape of the flame and the species production.

Pacheco et al. [10], using the same burner, developed some experiments on six different ammonia-hydrogen rich flames for a power input of 2800 W. Temperatures were measured for several points along the combustor axis and NO_x, NH_3 and H_2 emissions were measured in the flue gases. H_2 NH_3 unburnt were detected in high concentrations in the exhaust gases, and a spontaneous secondary flame was observed above the combustor due to unburnt reactants re-burning. A numerical analysis by using a Chemical Reactor Network (CRN) simplified model was also carried out for the clarification of the involved phenomena, through rate of production analysis.

The study here presented aims to follow the research pathway of these latter works. The strategy developed is the use of Chemical Reactor Network (CRN) model approach to predict and evaluate emissions from the considered burner fueled by a mixture of NH3/H2 under some conditions, using detailed chemistry modeling and in a fast way. Having that, the final target is to numerically evaluate the implementation of a Rich Quench Lean system to this burner, starting from the actual experimental apparatus.

2 Ammonia/hydrogen combustion

The stoichiometric idealized combustion of NH_3/H_2/air is given by Reaction 1, where x_{NH_3} represents the volume fraction of ammonia in the fuel.

$$(1-x_{NH_3})H_2 + x_{NH_3}NH_3 + (0.5+\frac{x_{NH_3}}{4})(O_2+3.76N_2) \rightleftharpoons (1+\frac{x_{NH_3}}{2})H_2O + (1.88+1.44x_{NH_3})N_2 \quad (1)$$

where x_{NH_3} is the volumetric fraction of NH_3 in the fuel mixture (Equation 2), which by assuming ideal gas approximation, is the same of NH_3 mole fraction in fuel.

$$x_{NH_3} = \frac{\dot{V}_{NH_3}}{\dot{V}_{NH_3} + \dot{V}_{H_2}} \quad (2)$$

where $\dot{V}_{NH_3}$ is the volumetric flow rate of NH_3 and $\dot{V}_{H_2}$ is the volumetric flow rate of H_2.

3 Experimental Setup

The experimental setup, firstly developed by Franco [2], is shown in Figure 1. Upstream of the burner mouth, marked with the red referential, a duct composed of two concentric tubes, being the inner tube for NH_3/H_2 supply and the outer for air swirling supply, conduct the reactants separately until 13.5 mm upstream the bluff-body where the fuel mixture is injected radially into the airflow through 12 holes of 2 mm diameter, promoting partial premixing at a short distance from the burner mouth. The bluff-body placed exactly at the burner mouth is shaped like a truncated cone, with a height of 20 mm, abase diameter of 22 mm, and a top diameter of 34 mm. Its function is to impede the passage of air/fuel flow by creating a recirculation zone in the flame downstream of the burner mouth. The combustor walls consist on a quartz tube, insulated with a layer of ceramic wool, surrounded by a reflective tape and finally covered by cylindrical stainless steels plates. In-flame measurements of temperature and species concentrations were previously performed for a wide range of flame conditions, along the central axis of the burner and at its exit [2, 3, 10].

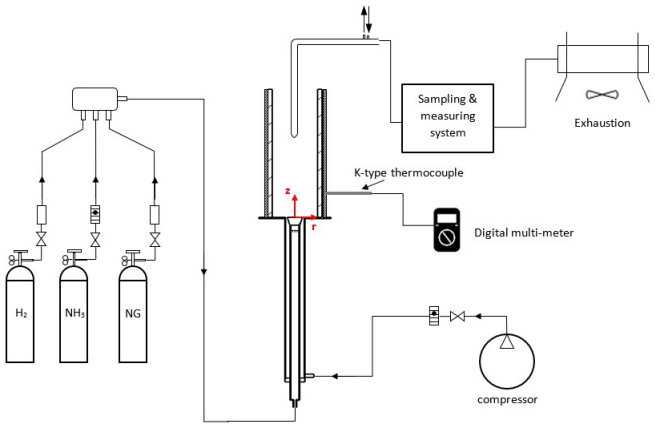

Figure 1: Schematic of the burner setup. Adapted from [2].

4 Model description

The kinetic modelling was performed with Cantera open-source software [5] (Python interface), an object-oriented package suitable for problems involving chemical kinetics of combustion. Cantera allows flexible network architecture of interconnected 0-dimensional reactors, with mass and heat exchange.

A chemical reactor network can be defined as a network of interconnect perfect mixing chemical reactors, or Perfectly Stirred Reactors (PSR), exchanging between them both mass and heat. The theoretical model of a PSR relies on the assumption of perfect mixing, which means an instantaneous mixing of the incoming reactants, fuel, and oxidant, which can therefore be considered homogeneous throughout the volume (fixed) of the reactor. Therefore, regardless of the intensity of turbulence mixing between reactants will always be assumed as perfect. Certain conditions must be met for CRN modelling to be used correctly in combustion. Combustion in turbulent premix flames and stabilized turbulent flame recirculation zones are conditions for which this approximation can be done [1]. The partially premixed turbulent flames obtained in the swirl and bluff-body stabilized burner from IDMEC can thus be candidates for CRN modelling. Previous studies [3, 11] on computational fluid dynamic (CFD) simulations, of type Large Eddy Simulation (LES) and

Reynolds Average Navier-Stokes (RANS) simulation, on flames under some conditions for this burner have already proposed flame division in distinct zones, distinguishing those where recirculation is a main concerning than others where the flame gas simply flows away in the same direction. These proposals were considered and further developed along the present work. The flame regions where recirculation exists were modelled by a PSR and those where the flow seems to be at a steady directional flow, with almost no recirculation, were modelled by a Plug Flow Reactor (PFR). Cantera library does not provide yet a specific class for PFR modelling, and thus PFR is implemented as a linear chain of PSRs.

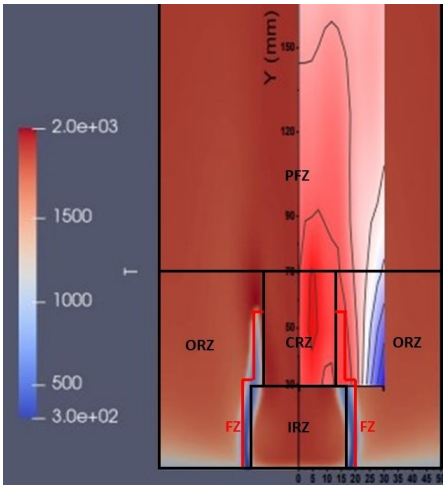

Figure 2: Reactors network in flame: $\phi = 0.8$, $x_{\mathrm{NH_3}} = 0.8$. Adapted from [11].

Five distinct regions were considered in this model as it is shown in Figure 2. The volumes of the reactors are assumed to be constant and fixed and their dimensions are estimated from RANS flame profiles. Although being an output of the simulation, it is expected that pressure would remain almost constant and equal to the atmospheric pressure. The Flame Zone (FZ) is the reactor modelling the flame front, where the incoming air and fuel first interact causing ignition. The Inner Recirculation Zone (IRZ) models the low velocity region at the downstream of the burner mouth promoted by the bluff-body, where combustion gases, mainly coming from FZ, recirculate. The Central Recirculation Zone (IRZ) models a second region with recirculation downstream the first one, where a considerable mass flow of hot gases remains for some residence time, recirculating and re-burning. The Outer Recirculation Zone (ORZ) models the region between the flame front and the quartz tube wall with high concentration of air and some residual recirculating combustion products, and where some radicals reactions are expected to occur, but not combustion, due to low temperatures and fuel absence. The Post-Flame Zone (PFZ), the larger one and just upstream the combustor exit, models the flame region where the gases resulting from combustion simply flow, in a continuous and steady way, taking place some relevant reactions. In Cantera, the first mentioned four zones were modelled by PSRs while the PFZ was modelled by a PFR.

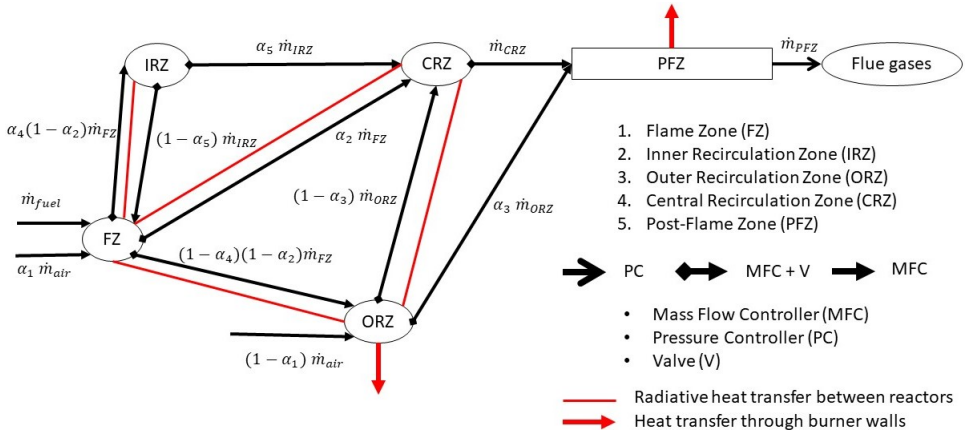

Figure 3: Diagram for the CRN model of a single-stage swirl and bluff-body burner type.

Figure 3 shows a schematic diagram with the final model diagram of the single-stage combustor, being also represented the considered heat and mass transfer interactions between reactors and its surroundings. In Cantera, the mass flow trajectory between two reactors is implemented using Mass Flow Controllers (MFC), Pressure Controllers (PC) and Valves (V) [5]. Using MFC the mass flow rates are imposed following Equations 3-7, and V are used in parallel with MFC to assure minimum pressure differences between neighboring reactors.

Regarding mass transfer within the interconnected reactors, the first to attain is mass conservation, for which some network mass splitting coefficients must be defined, α_1 to α_5. They consist on the mass flow fraction entering or exiting a reactor (Figure 3), given by Equations 3 to 7. The value for each one of those coefficients was found from a parametric adjustment work of the numerical results, for a certain combination of coefficients, with the experimental ones available for the same input conditions. The adjustment was done by evaluating average relative errors between numerical and experimental results, allied with visual inspecting of the results trends. For future work it is highly recommended an optimization of this process, by defining and implementing an objective function. The best fitting with temperature and with oxygen (a major species) experimental profiles was the main criteria to consider satisfactory the set of coefficients used. After the adjustment procedure it was verified a similarity in the flow split coefficients for different flames. This was consider reasonable due to the similar flow velocities of the different flames analyzed [2, 10].

$$\dot{m}_{FZ} = \alpha_1 \, \dot{m}_{air} + \dot{m}_{fuel} \tag{3}$$

$$\dot{m}_{ORZ} = (1-\alpha_1) \, \dot{m}_{air} + (1-\alpha_4)(1-\alpha_2) \, \dot{m}_{FZ} \tag{4}$$

$$\dot{m}_{IRZ} = \alpha_4 (1-\alpha_2) \, \dot{m}_{FZ} \tag{5}$$

$$\dot{m}_{CRZ} = \alpha_2 \, \dot{m}_{FZ} + \alpha_5 \, \dot{m}_{IRZ} + (1-\alpha_3) \, \dot{m}_{ORZ} \tag{6}$$

$$\dot{m}_{PFZ} = \dot{m}_{air} + \dot{m}_{fuel} \tag{7}$$

The residence time in each reactor, given by Equation 8, will be a function of these coefficients α_1 to α_5 since the volume of each reactor is constant and the gas density in the reactor is calculated by solving the ODEs of the reacting system.

$$t_r = \rho V / \dot{m} \tag{8}$$

Regarding heat transfer, Equation 9 establishes the heat exchange occurring between reactors or between one reactor and the exterior environment.

$$\dot{Q} = UA(T_{left} - T_{right}) + \varepsilon \sigma A(T_{left}^4 - T_{right}^4) + A q_0(t) \tag{9}$$

where U is an overall heat transfer coefficient in $W/(m^2K)$, A is the heat transfer area in m^2, ε is the wall emissivity, σ is the Stefan-Boltzmann radiation constant, and $q_0(t)$ is a time-dependent heat flux in W/m^2 (not accounted in this work). The overall heat transfer exchanged with exterior surroundings through combustor wall was estimated using geometry, materials and temperatures known, and the interval of 5-11 $W/(m^2K)$ was considered a reasonable range for this value. In a previous work Franco et al. [3], it was assumed an overall heat transfer coefficient (U_{ovr}) of 10 $W/(m^2K)$ for LES modelling.

Having considered only heat transfer between the exterior environment and the reactors in contact with the tube wall, some disparity in temperatures and compositions for some neighboring reactors suggested the need to model the heat transfer taking place between these reactors. This heat transfer was modeled by assuming radiation between walls of reactors in contact, considering emissivity values for flame radiation, ε_f. Although perhaps a crude approximation it proved to improve final results, comparing with those obtained without using this strategy. Although the still scarce available information on radiative heat transfer phenomena in ammonia flames it can be foreseeing a reasonable range of values for emissivity in NH_3/H_2 flames similar to those of H_2 or biomass flames, mainly due to the high water vapor molar fraction. It was considered the range of 0.1 to 0.25 a reasonable one for NH_3/H_2 flame emissivity. Given these reference ranges for both U_{ovr} and ε_f, those values were also checked with a parametric study to assure the better fitting of final model results to the experimental ones. For future a better heat transfer model of the present burner should be developed. After a fitting parametric treatment, the selected coefficients are gathered in Table 1.

The output results given by the simulation performed with the model consist on tracking temperature and species mole fraction values along several points over the central axis of the burner (profile) from 30 *mm* to 300 *mm*. This region in the flame is modeled by IRZ (1 point), CRZ (1 point) and PFZ (N_{PSR} points), and thus results from those zones will compose the profiles. The relative error associated with the profiles is obtained by Equation 10, where x_i are the measure value at each position both for experimental (e) and numerical (n) profiles. Since the number of experimental

		Model Coefficients							
		U_{ovr}	ε	α_1	α_2	α_3	α_4	α_5	N_{PSR}
Flame 1	Lean	7.5	0.2	0.97	0.9	0.9	0.9	0.99	100
	Stoich.	11	0.2	0.99	0.9	0.9	0.9	0.99	100
Flame 2	Lean	7.5	0.2	0.99	0.9	0.9	0.9	0.99	100
	Rich	9.5	0.2	0.97	0.9	0.9	0.9	0.99	100
Flame 3	Lean	7.5	0.2	0.98	0.9	0.9	0.9	0.99	100
	Rich	8.5	0.2	0.97	0.9	0.9	0.9	0.99	100
Flame 4	Lean	7.5	0.2	0.98	0.9	0.9	0.9	0.99	100
	Stoich.	11.5	0.2	0.99	0.9	0.9	0.9	0.99	100
Flame 5	Lean	7.5	0.2	0.98	0.9	0.9	0.9	0.99	100
	Rich	10	0.2	0.97	0.9	0.9	0.9	0.99	100
Flame 6	Lean	-	-	-	-	-	-	-	-
	Rich	8.5	0.2	0.97	0.9	0.9	0.9	0.99	100

Table 1: Model coefficients for the better fitting with experimental temperature and species concentrations profiles.

measurements is different from the number of reactors in PFZ, an interpolation was done to calculate numerical values for the same position of the experimental ones, to improve the performance of the error evaluation.

$$RAE_{profile}[\%] = \frac{\sum_i^N |x_i^{(e)} - x_i^{(n)}|}{N_e \times \overline{x}^{(e)}} \times 100 \tag{10}$$

The relative error (RE) for numerical results at the exit of the burner, as well as for IRZ and CRZ results, is given by Equation 11.

$$RE_{exit}[\%] = \frac{|x_{exit}^{(e)} - x_{exit}^{(n)}|}{x_{exit}^{(e)}} \times 100 \tag{11}$$

Figure 4 shows the diagram of the RQL system, being adapted from that of the single-stage combustor by adding a secondary stage consisting on the Quench Zone (QZ) and the Lean Zone (LZ). The first stage, consisting on that of the single-stage burner will be operate in rich regime and thus will be the Rich Zone (RZ). In the RQL model, a secondary incoming air mass flow rate enters the QZ, where rapid mixing and cooling happens, promoted by the meeting of incoming air and effluent gases from RZ. The resulting mixture then flows through LZ.

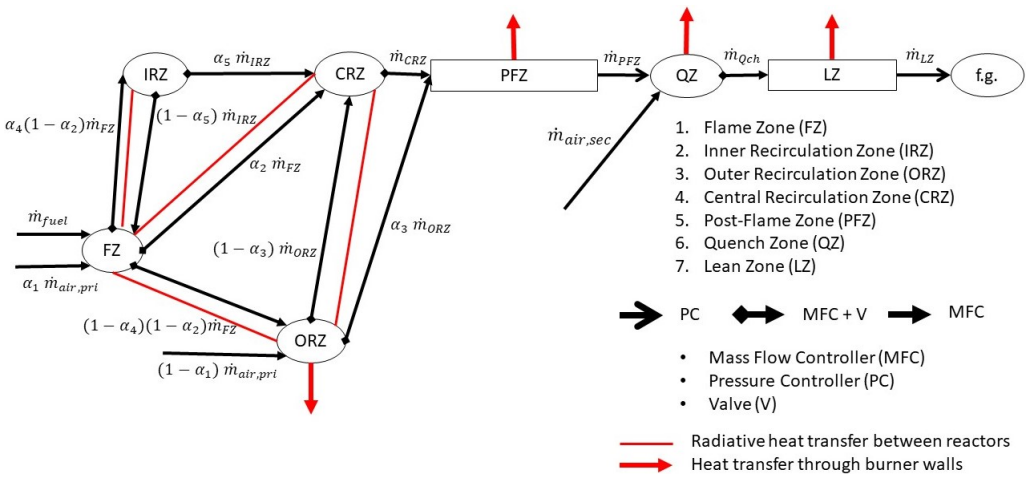

Figure 4: Diagram for the CRN model of a swirl and bluff-body burner adapted to RQL type combustor.

4.1 Numerical test conditions

The test conditions used as model inputs are exposed in Table 2. Mass flow rates were theoretically calculated as function of the thermal input, TI, the equivalence ratio, ϕ, and the NH_3 volume fraction in the fuel, x_{NH_3}.

For the chemical kinetics modelling two detailed mechanisms were selected to a comparison work: Glarborg at al. [4] and Stagni et al. [12]. Having used several mechanisms [4, 6, 7, 8, 9, 12], the Stagni mechanism was the one with closest predictions to experiments. The Glarborg mechanism was selected due to its well known comprehensiveness of nitrogen chemistry processes, and to test the speed of a simulation with a very detailed mechanism.

		Initial Conditions						
		$TI\ [W]$	x_{NH_3}	ϕ	$\dot{m}_{air}\ [kg/s]$	$\dot{m}_{NH_3}\ [kg/s]$	$\dot{m}_{H_2}\ [kg/s]$	$V\ [m/s]$
Flame 1	Lean	1900	0.7	0.8	7.539e-04	7.693e-05	3.911e-06	3.50
	Stoich.	2800	0.7	1.0	8.888e-04	1.134e-04	5.763e-06	4.33
Flame 2	Lean	1900	0.8	0.8	7.626e-04	8.575e-05	2.543e-06	3.52
	Rich	2800	0.7	1.1	8.080e-04	1.134e-04	5.763e-06	4.03
Flame 3	Lean	1900	0.9	0.7	8.809e-04	9.415e-05	1.241e-06	3.94
	Rich	2800	0.7	1.2	7.407e-04	1.134e-04	5.763E-06	3.78
Flame 4	Lean	1900	0.9	0.8	7.708e-04	9.415E-05	1.241E-06	3.53
	Stoich.	2800	0.8	1.0	8.990e-04	1.264E-04	3.747E-06	4.35
Flame 5	Lean	1900	0.9	0.9	6.851e-04	9.415E-05	1.241E-06	3.21
	Rich	2800	0.8	1.1	8.173e-04	1.264E-04	3.747E-06	4.04
Flame 6	Lean	-	-	-	-	-	-	-
	Rich	2800	0.8	1.2	7.492e-04	1.264E-04	3.747E-06	3.79

Table 2: Operating conditions theoretically obtained for each flame analyzed.

5 Results and discussion

Results predicted by the model are captured from the IRZ (30 mm), CRZ (70 mm), and the various reactors that form the chain that models the PFZ (70 mm to 300 mm). The line connecting IRZ and CRZ, in the graphs, does not intend to model the evolution between the two zones. Numerical results were obtained for the two selected chemical kinetics mechanisms, Glarborg and Stagni. For the lean flames there are experimental results for temperatures and mole fractions of NO_x and O_2 (dry volume) for various points along the central axis of the burner. For stoichiometric and rich flames, there are only measurements of temperatures for various points along the central axis of the burner, and measurements of NO_x, NH_3 and H_2 emissions in the flue gases, measured at the burner exit.

5.1 Validation against experimental data

Figure 5 brings together the numerical predictions of the temperature profiles and molar fractions of the main species, compared to the respective experimental results, for the five lean flames analyzed. For all cases, the trends in the profiles due to the variation of ϕ and x_{NH_3} are verified. A close examination of the behavior of the profiles observed in Figure 5c allows one to conclude that the model predictions are quite close to complete combustion, since flames for different values of x_{NH_3} show very close profiles, and it is theoretically predicted for the ideal case of complete combustion that the mole fraction of O_2 is independent of x_{NH_3}, and only dependent on x_{NH_3}, as indeed is also seen in the plot of Figure 5d. The predicted NO_x mole fractions show a quite significant NO_x overproduction compared to the experimentally measured values, and quite different predictions for the two mechanisms. Furthermore, it is not predicted the gradual decrease in NO_x mole fraction along the flame, as shown by the experimental results. The fact that almost complete burning of the ammonia occurs too early in the model, in the FZ, mainly due to the perfect mixing assumption, prevents a sufficient flow of ammonia from entering the IRZ, CRZ and PFZ, to the enabling of the SNCR reactions. These reactions seem to be the main responsible for the decrease in NO_x in the experimental flame, but are not being predicted by the model.

Figure 6 shows the comparison between numerical and experimental for the analyzed stoichiometric and rich flames. Also for these flames, the trends observed experimentally with the variation of x_{NH_3} and with ϕ are also verified by the numerical results. Both mechanisms generally predict excess NO_x compared to experimental tests, although the numerical results with the Stagni mechanism are particularly close to the experimental ones, especially for $\phi = 1.0$ and $\phi = 1.2$. The NO_x sharp decreasing particularly for flames with higher ϕ shows how the developed model is able to account for NO reduction reactions as long as the necessary conditions for them to happen are met, which are basically the presence of NO_x and sufficient amounts of unburned NH_3. Ammonia cracking into hydrogen for the richer flames is demonstrated by the slight increase in H_2 at the entrance to the PFZ (70 mm), exactly at the same point where a relatively sharp decrease was observed for the NH_3 profiles of the respective flames.

5.2 Parametric studies for RQL model

Figure 7a presents the impact of varying the ϕ_{pri} parameter on the main pollutant emissions for $x_{NH_3} = 0.8$, $\phi_{ovr} = 0.8$ and $L_{QZ} = 20\,mm$ and $TI = 2800\,W$. Both mechanisms point to a minimum, and therefore optimal among those considered, level of NO_x emissions for relatively close values of ϕ_{pri}: 1.1 for the Stagni mechanism and 1.2 for the Glarborg

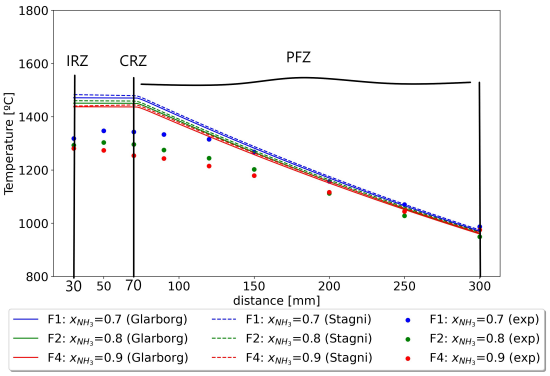

(a)

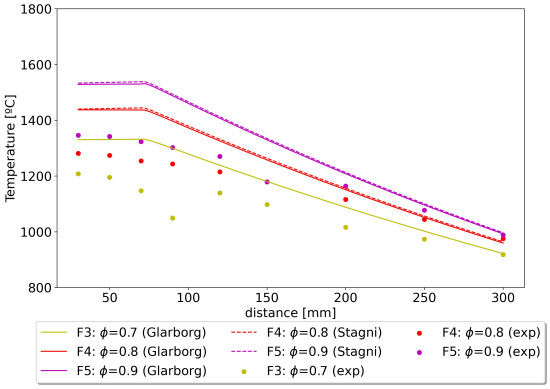

(b)

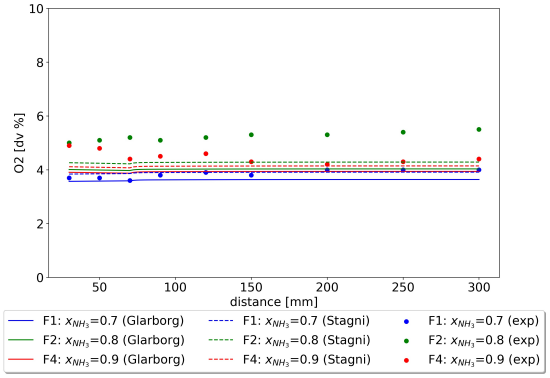

(c)

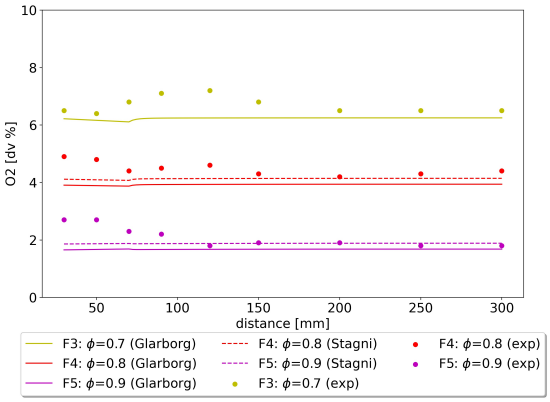

(d)

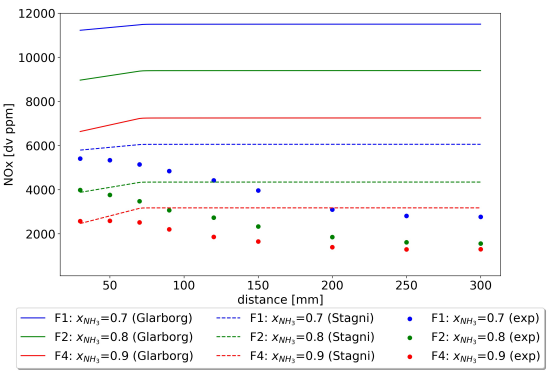

(e)

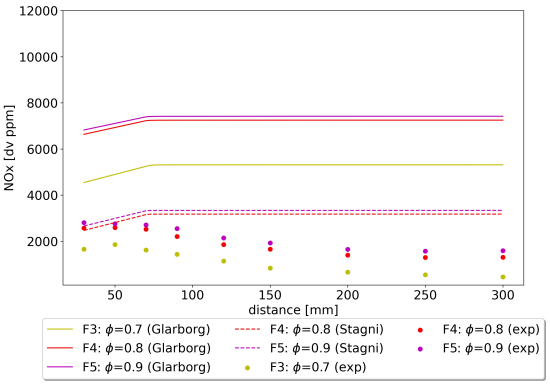

(f)

Figure 5: Numerical and experimental temperature and species profiles in lean flames along the combustor. Left column: $\phi = 0.8$. Right column: $x_{\mathrm{NH_3}} = 0.9$.

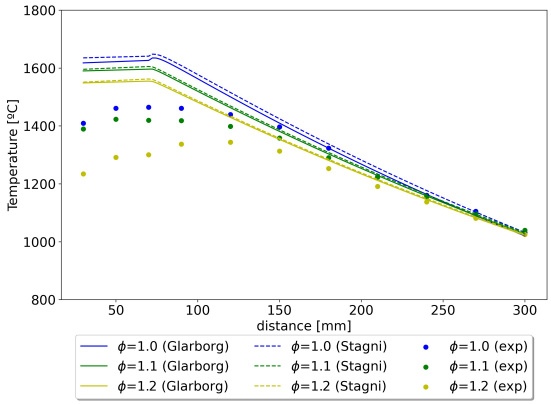

(a)

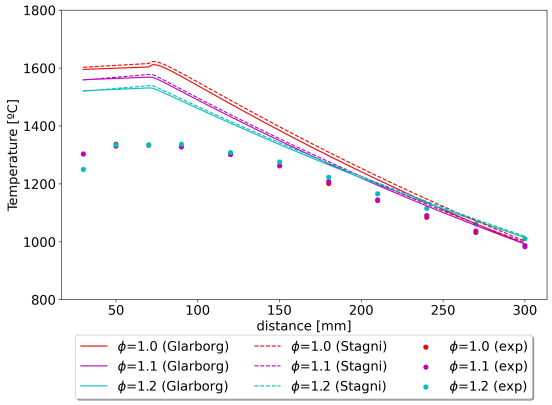

(b)

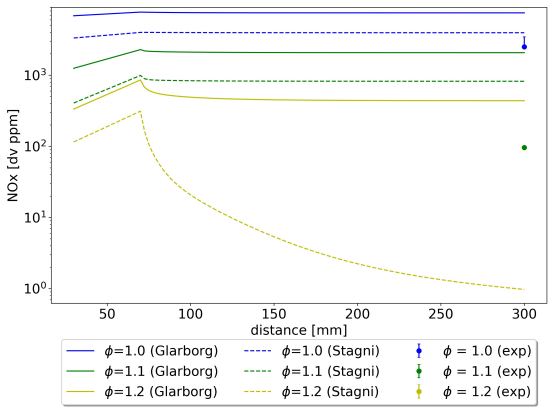

(c)

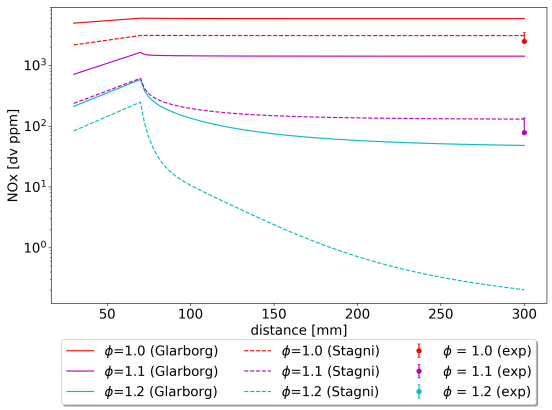

(d)

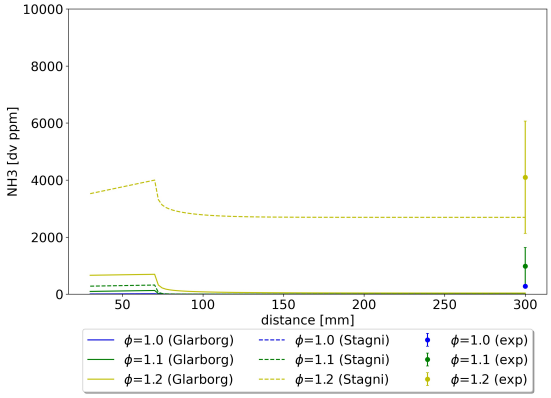

(e)

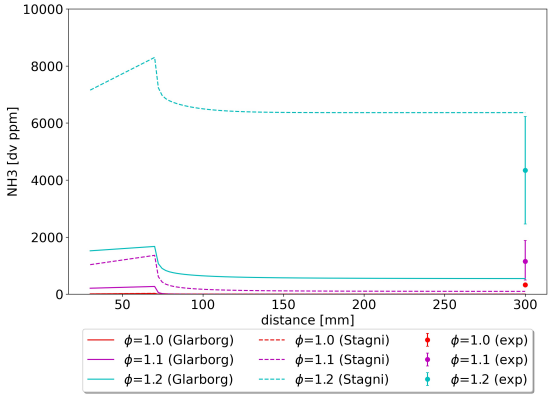

(f)

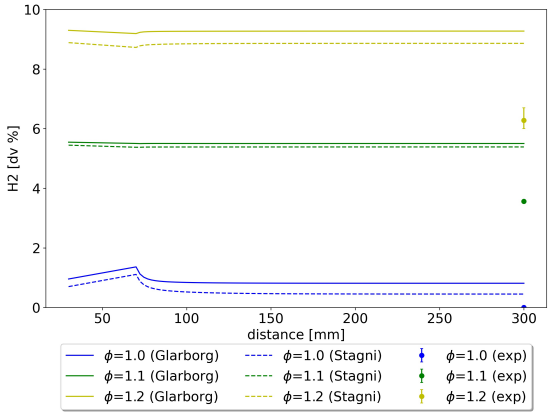

(g)

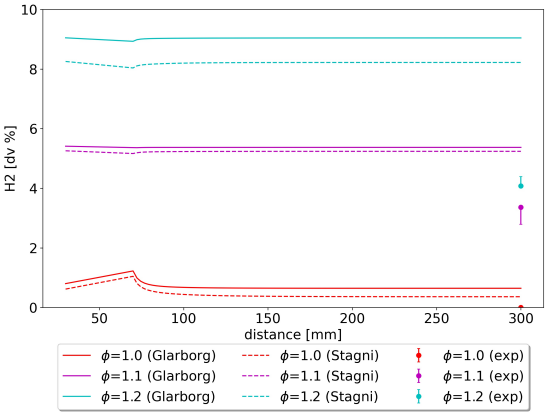

(h)

Figure 6: Numerical and experimental temperature and species profiles in stoich. and rich flames along the combustor. Left column: $x_{NH_3} = 0.7$. Right column: $x_{NH_3} = 0.8$.

mechanism. From a certain equivalence ratio, it can be seen how the NO_x production particularly occurs in the lean stage, through the conversion of unburnt NH_3 via the fuel-NO pathway, and thus increasing the NO_x level with the increasing equivalence ratio. Regarding SNCR reactions, it can also be pointed out the these reactions may be a main reason for the observed concave downward curve of NO_x emissions with the increasing of the equivalence ratio, since the increasing of unburnt mole fraction of NH_3 in lean stage may enhance those reactions for the NO_x reduction.

The predicted impact of the ϕ_{ovr} parameter on the emissions at the exit of the RQL system can be analyzed using Figure 7b, for $x_{NH_3} = 0.8$, $\phi_{pri} = 1.2$ and $L_{QZ} = 20\ mm$ and $TI = 2800\ W$. From the predicted value of ϕ_{ovr} at which ignition occurs, both mechanisms agree in predicting increasing NO_x concentration in the flue gas for increasing equivalence ratio, with the Stagni mechanism being the one that predicts higher values. This increase seems to be especially associated with the temperature increase that occurs as the stoichiometry approaches, so that the main pathway of NO_x production should be the thermal-NO mechanism.

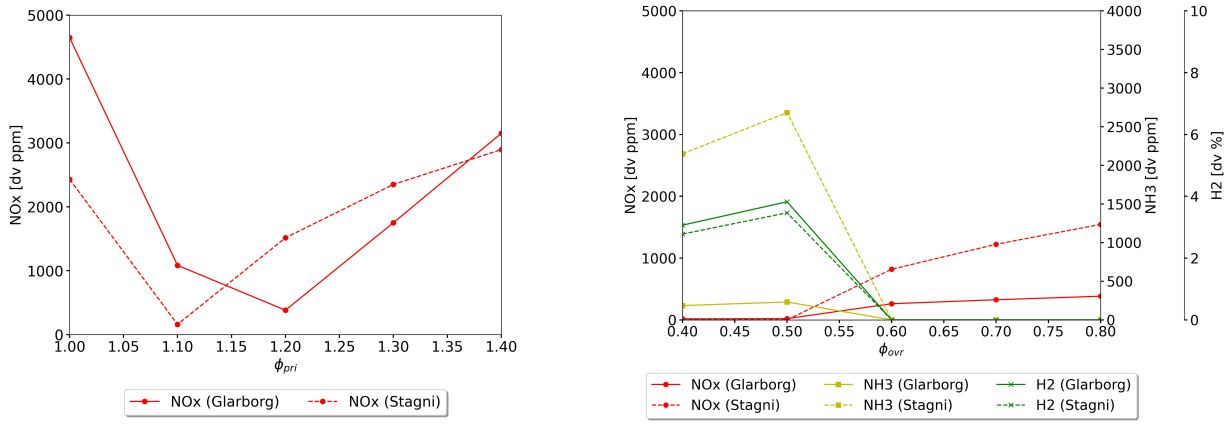

(a) (b)

Figure 7: Flue gas emissions for RQL model. Initial conditions: $TI = 2800\ W$, $x_{NH_3} = 0.8$, $L_{QZ} = 20\ mm$ and (a) $\phi_{ovr} = 0.8$ and (b) $\phi_{pri} = 1.2$.

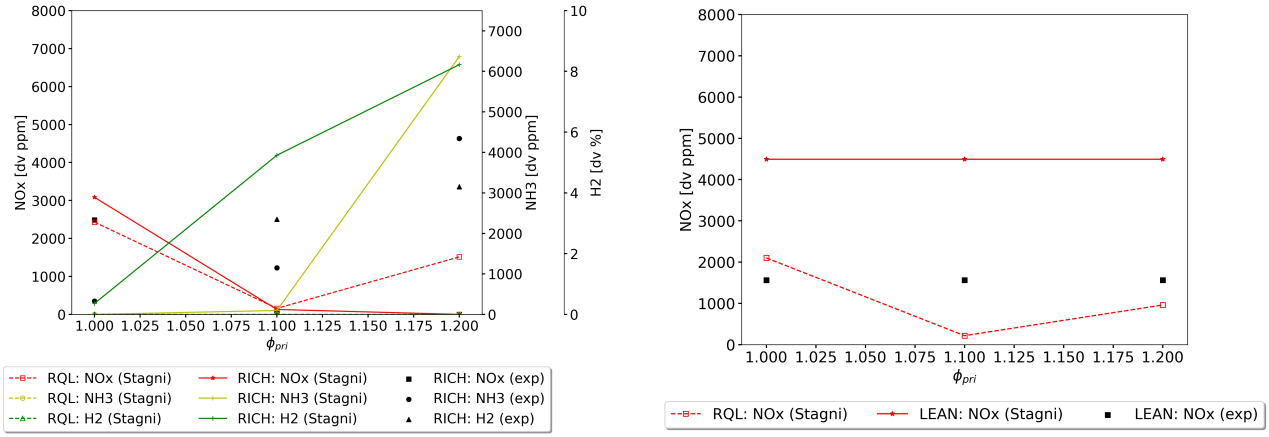

(a) (b)

Figure 8: Flue gas emissions for experimental and numerical single rich stage versus RQL. Initial conditions: , $x_{NH_3} = 0.8$, $\phi_{ovr} = 0.8$, $L_{QZ} = 20\ mm$ and (a) $TI = 2800\ W$ and (b) $TI = 1900\ W$.

5.3 RQL model predictions against single-stage combustor

Comparing the predicted emissions for the RQL burner with the experimental and the predicted emissions for the single-stage rich burner, in Figure 8a, it can be observed an optimal operation point, for $\phi = 1.1$, where NO_x reaches a minimum value, being both NH_3 and H_2 emissions null at the exit of the RQL. This points to the main advantage of RQL implementation in comparison with a single rich stage, both enhancing combustion efficiency and assuring very low emissions.

From the comparison between predicted RQL flue gas results with those for the numerical and experimental single lean stage with the same ϕ_{ovr}, shown in Figure 8b, it is possible to directly conclude that the prediction values seems to corroborate the effectiveness of the RQL system in terms of NO_x emissions reduction. NH_3 and H_2 emissions are null for both single lean stage and RQL system.

6 Summary

The following main conclusions may summarize the accomplishments of this work:

- The chemical reactor network model developed proved to correctly predict the trends of all profiles with the variation of ϕ, x_{NH_3} and TI, in accordance with the same trends presented in the experimental.
- The model have frequently shown over-predicted values of NH_3 conversion, leading to over-prediction of NO_x mole fractions as well as H_2 mole fraction from NH_3 cracking.
- According to the developed model, the implementation of a Rich-Quench-Lean system in the current burner would be advantageous regarding the reduction of NO_x, NH_3 and H_2 emissions, for the best predicted conditions of $x_{NH_3} = 0.8$, $\phi_{ovr} = 0.7$, $\phi_{pri} = 1.1 - 1.2$.
- The effectiveness of using the RQL combustor concept with respect to pollutant emissions depends mainly on the parameter ϕ_{pri}, with emissions being minimal for a specific value of this parameter, which is confirmed by the literature. According to the predictions of the developed model this value is close to 1.1.
- The best ϕ_{ovr} to be used in the RQL system for minimizing pollutant emissions is the minimum value from which ignition in the Lean stage can be guaranteed.

References

[1] P. Coelho and M. Costa. *Combustão*. Ed. by Edições Orion. 2ª Edição Revista. Feb. 2012. ISBN: 978-972-8620-10-3.

[2] Miguel Alexandre Coelho Franco. "Ammonia combustion on a swirl and bluff body stabilized burner". MA thesis. Instituto Superior Técnico, ULisboa, 2020.

[3] Miguel C. Franco et al. "Characteristics of NH3/H2/air flames in a combustor fired by a swirl and bluff-body stabilized burner". In: *Proceedings of the Combustion Institute* 38.4 (2021), pp. 5129–5138.

[4] P. Glarborg et al. "Modeling nitrogen chemistry in combustion". In: *Progress in Energy and Combustion Science* 67 (2018), pp. 31–68.

[5] David G. Goodwin et al. *Cantera: An Object-oriented Software Toolkit for Chemical Kinetics, Thermodynamics, and Transport Processes*.

[6] S. J. Klippenstein et al. "The role of NNH in NO formation and control". In: *Combustion and Flame* 158.4 (2011), pp. 774–789.

[7] R. Li et al. "Chemical mechanism development and reduction for combustion of NH3/H2/CH4 mixtures". In: *Fuel* 257 (2019), p. 116059.

[8] H. Nakamura, S. Hasegawa, and T. Tezuka. "Kinetic modeling of ammonia/air weak flames in a micro flow reactor with a controlled temperature profile". In: *Combustion and Flame* 185 (2017), pp. 16–27.

[9] J. Otomo et al. "Chemical kinetic modeling of ammonia oxidation with improved reaction mechanism for ammonia/air and ammonia/hydrogen/air combustion". In: *International Journal of Hydrogen Energy* 43.5 (2018), pp. 3004–3014.

[10] Gonçalo P. Pacheco et al. "Experimental and Kinetic Investigation of Stoichiometric to Rich NH3/H2/Air Flames in a Swirl and Bluff-Body Stabilized Burner". In: *Energy & Fuels* 35.9 (2021), pp. 7201–7216.

[11] R. C. Rocha et al. "Numerical and experimental characterization of partially premixed NH3/H2/air flames on a laboratory scale combustor".

[12] A. Stagni et al. "An experimental, theoretical and kinetic-modeling study of the gas-phase oxidation of ammonia". In: *React. Chem. Eng.* 5 (4 2020), pp. 696–711.